Journal of Colloid and Interface Science 480 (2016) 102–108

Contents lists available at ScienceDirect

Journal of Colloid and Interface Science

journal homepage: www.elsevier.com/locate/jcis

Regular Article

Transient aggregation of chitosan-modified poly(D,L-lactic-co-glycolic) acid nanoparticles in the blood stream and improved lung targeting efficiency

Song Yi Lee [a], Eunjae Jung [b], Ju-Hwan Park [b], Jin Woo Park [c], Chang-Koo Shim [b], Dae-Duk Kim [b], In-Soo Yoon [c,*], Hyun-Jong Cho [a,**]

[a] College of Pharmacy, Kangwon National University, Chuncheon 200-701, Republic of Korea
[b] College of Pharmacy and Research Institute of Pharmaceutical Sciences, Seoul National University, Seoul 151-742, Republic of Korea
[c] College of Pharmacy and Natural Medicine Research Institute, Mokpo National University, Jeonnam 534-729, Republic of Korea

GRAPHICAL ABSTRACT

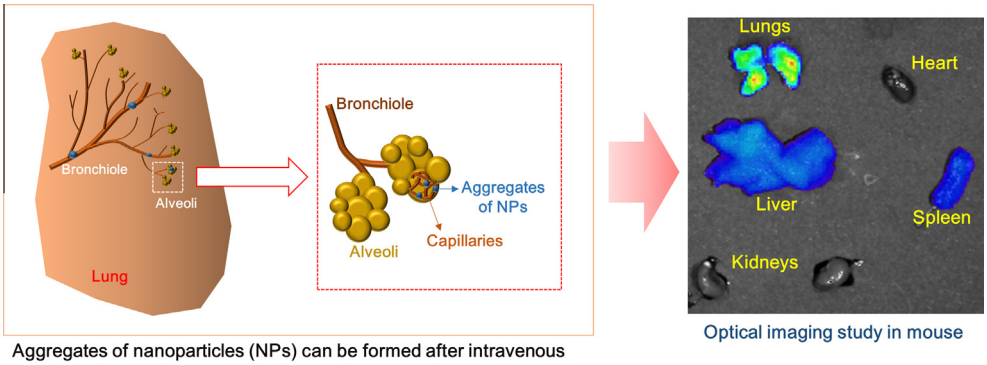

Aggregates of nanoparticles (NPs) can be formed after intravenous administration and entrapped in the capillary bed of lungs.

ARTICLE INFO

Article history:
Received 8 June 2016
Revised 4 July 2016
Accepted 5 July 2016
Available online 6 July 2016

Keywords:
Chitosan
Intravenous injection
Lung targeting
Nanoparticles
PLGA
Transient aggregation

ABSTRACT

Chitosan (CS)-modified poly(D,L-lactic-co-glycolic) acid (PLGA) nanoparticles (NPs) were prepared and their lung targetability after intravenous administration was elucidated. PLGA NPs (mean diameter: 225 nm; polydispersity index: 0.11; zeta potential: −15 mV), 0.2% (w/v) CS-coated PLGA NPs (CS02-PLGA NPs, mean diameter: 264 nm; polydispersity index: 0.17; zeta potential: −7 mV), and 0.5% (w/v) CS-coated PLGA NPs (CS05-PLGA NPs, mean diameter: 338 nm; polydispersity index: 0.23; zeta potential: 12 mV) were fabricated by a modified solvent evaporation method. PLGA NPs maintained their initial particle size in different media, such as human serum albumin (HSA) solution, rat plasma, and distilled water (DW), while CS05-PLGA NPs exhibited the formation of aggregates in early incubation time and disassembly of those into the NPs in late incubation time (at 24 h). According to the sodium dodecyl sulfate-polyacrylamide gel electrophoresis (SDS-PAGE) analysis, the binding affinity of CS05-PLGA NPs with HSA and rat plasma was higher than that of PLGA NPs. By a near-infrared fluorescence (NIRF) imaging test in the mouse, the selective accumulation of CS05-PLGA NPs, rather than PLGA NPs, in lung tissue was demonstrated. These findings suggest that CS05-PLGA NPs can form transient aggregates in the blood

* Corresponding author.
** Corresponding author.
E-mail addresses: isyoon@mokpo.ac.kr (I.-S. Yoon), hjcho@kangwon.ac.kr (H.-J. Cho).

http://dx.doi.org/10.1016/j.jcis.2016.07.006

stream after intravenous administration and markedly improve lung targeting efficiency, compared with PLGA NPs.

1. Introduction

During the past decades, polymeric nanoparticles (NPs) have been extensively investigated as drug delivery systems because of their capabilities to improve drug stability, cellular uptake efficiency, and targetability to specific tissues and organs [1–5]. Among various polymers as a matrix of NPs, poly(D,L-lactic-co-glycolic) acid (PLGA) has been approved for clinical uses due to its biocompatibility and biodegradability [6]. Although a great number of researches have shown the feasibility of PLGA NPs for organ and tissue-specific drug delivery, most of them were insufficient for achieving clinically significant therapeutic outcomes [7,8]. Thus, to further improve the biological functions of PLGA NPs, previous studies have adopted various approaches including chemical conjugation with functional groups or physical mixing with various materials [9].

As one of surface-functionalized NPs, chitosan (CS)-coated NPs have been widely investigated for drug delivery [2,10–12]. CS is a cationic polyelectrolyte composed of β(1 → 4) linked glucosamine and *N*-acetyl-D-glucosamine. It is a biocompatible and biodegradable polymer, which can be obtained by the partial deacetylation of chitin, primarily derived from crustacean and insect shells [13]. In general, cationic NPs tend to be favorable for endocytosis mainly based on the electrostatic interactions with negatively charged cellular membranes [14]. In addition, CS is one of mucoadhesive polymers and it can enhance cellular permeability in a reversible and dose-dependent manner [15].

CS-modified PLGA NPs have been investigated based on the strong electrical interaction between positively charged CS and negatively charged PLGA NPs. In our previous study [16], CS-modified PLGA NPs containing paclitaxel were fabricated and that group exhibited higher lung concentrations of paclitaxel in normal mice after intravenous injection, compared with unmodified PLGA NPs and Taxol groups. It was speculated that these results could be related to the transient aggregation of CS-modified PLGA NPs in the blood stream followed by an enhanced distribution in the lung capillary. However, no direct evidence was provided in that study [16], thus *in vivo* fate and lung targetability of CS-modified PLGA NPs are further elucidated in this investigation.

Although micro-sized carriers have been used for the delivery of drug *via* pulmonary route [17,18], micro-sized particles administered intravenously also can be accumulated in the lung thus they can be used for lung-targeted drug delivery [19–23]. It is known that microparticles (MPs) can have an enhanced passive pulmonary targeting and improved retention in the lungs [24]. However, MPs can induce embolization and unwanted toxicities after intravenous injection. To overcome these drawbacks, spontaneously formed micro-sized aggregates composed of NPs (as a block unit) were designed and their lung targetability was demonstrated in this study. Particularly, particle size alteration of NPs in the media containing blood components, adsorption of proteins onto the surface of NPs, and *in vivo* fate of NPs by a real-time optical imaging were investigated.

2. Materials and methods

2.1. Materials

CS (molecular weight [MW]: 45–50 kDa; deacetylation degree: 75–80%), PLGA (MW: 40–75 kDa; lactide/glycolide: 50/50), and polyvinyl alcohol (PVA; MW: 67 kDa) were purchased from Sigma–Aldrich Co. (St. Louis, MO, USA). Cy5.5 (FKR-675) was obtained from BioActs (Incheon, Korea). All other chemicals and reagents were analytical grade and were obtained from commercial sources.

2.2. Preparation and characterization of NPs

PLGA NPs were fabricated using a modified emulsification-solvent evaporation method [25,26]. Briefly, PLGA (30 mg) was solubilized in dichloromethane (1.5 mL) and that solution was added to 15 mL PVA solution (0.5%, w/v). That oil-in-water type emulsion was sonicated for 10 min using a probe sonicator (VC-750; Sonics & Materials, Inc., Newtown, CT, USA). The organic solvent was then removed by stirring for 1 h at room temperature. That dispersion of NPs was centrifuged at 13,200 rpm for 30 min and the supernatant was removed. The pellets of NPs were then resuspended with distilled deionized water (DDW; 1.8 mL). Those centrifugation and resuspension steps were repeated at least three times to eliminate residual PVA completely. For storage, the dispersion of NPs was freeze-dried after adding 3% (w/v) sucrose (as a cryoprotectant).

For preparing CS-PLGA NPs, PLGA NPs were fabricated as described above. Residual amount of PVA was completely removed by at least 3 cycles of resuspending and centrifuging steps. After obtaining the pellet of NPs, it was resuspended with 0.2% (w/v) or 0.5% (w/v) CS solution (1.5 mL) including 1% (w/v) acetic acid to fabricate 0.2% (w/v) CS-coated PLGA NPs (CS02-PLGA NPs) and 0.5% (w/v) CS-coated PLGA NPs (CS05-PLGA NPs). That dispersion of NPs was centrifuged at 13,200 rpm for 30 min again and resuspended with DDW (1.8 mL). NPs were also lyophilized after adding 3% (w/v) sucrose for further uses.

The particle size, polydispersity index, and zeta potential of prepared NPs were measured using dynamic light scattering (DLS) and laser Doppler methods (ELS-Z1000; Otsuka Electronics, Tokyo, Japan).

For monitoring the aggregation of NPs in different media, the dispersion of NPs in DDW was mixed with HSA solution (20 mg/mL), rat plasma, and DDW at 1:1 volume ratio. Then, that mixture was incubated at 37 °C for 24 h. At 0, 15, 30, 60, 120, and 1440 min, the particle size of each sample was measured by DLS method (ELS-Z1000; Otsuka Electronics, Tokyo, Japan).

The morphological shapes of PLGA NPs and CS05-PLGA NPs were observed using a variable pressure-field emission-scanning electron microscope (VP-FE-SEM; SUPRA 55VP, Carl Zeiss, Germany). Aliquots of NPs were mounted on stubs, coated with Pt under vacuum, and observed by VP-FE-SEM.

2.3. Sodium dodecyl sulfate-polyacrylamide gel electrophoresis (SDS-PAGE) analysis

The dispersion of NPs in DDW (0.5 mL) was mixed with aliquot (0.5 mL) of HSA solution (20 mg/mL), rat plasma, or DDW. After incubating for 24 h at 37 °C, the mixture of the dispersion of NPs and media was centrifuged for 30 min at 13,200 rpm. Supernatant was discarded and the NP pellet was resuspended with DW (1 mL). After mixing suspension (10 μL) and sample buffer (10 μL), that mixture was loaded into the gel. The binding patterns of proteins to NPs were assessed by SDS-PAGE. Gel electrophoresis was conducted using 10% running gel and 5% stacking gel by Laemmli's

discontinuous method [27]. HSA (20 μg) and rat plasma were loaded to each well alone or with NPs. Gels were run for 80 min at 120 V. After electrophoresis, the gel was stained with Coomassie R-250 staining solution (Bio-Rad Laboratories, Inc., Hercules, CA, USA) for 30 min and it was destained overnight.

2.4. Optical imaging

In vivo biodistribution of developed NPs in mouse was evaluated by a real-time near-infrared fluorescence (NIRF) imaging. Cy5.5-loaded PLGA NPs and CS05-PLGA NPs were fabricated for NIRF imaging. Cy5.5 (0.1 mg) was incorporated into the PLGA (30 mg) NPs according to the described method in Section 2.2. CS05-PLGA NPs were fabricated by coating PLGA NPs with 0.5% (w/v) CS. The content of Cy5.5 in NPs was quantitatively determined by the measurement of absorbance at 680 nm using an EMax Precision Microplate Reader (Molecular Devices, Sunnyvale, CA, USA).

Female BALB/c nude mice (5-weeks-old, Charles River, Wilmington, MA, USA) were used for NIRF imaging study. Mice were maintained in a light-controlled room maintained at 22 ± 2 °C and 55 ± 5% relative humidity. The experimental procedures were approved by the Animal Care and Use Committee of the College of Pharmacy, Seoul National University. Dispersion (0.1 mL) of NPs including 200 μg/kg dose of Cy5.5 was injected to the tail vein of the mice and they were anesthetized by inhalation of isoflurane (2.5%) before whole body scanning by Spectral Lago X (Spectral Instruments Imaging; Tucsan, AZ, USA). AMIView software (ver. 1.7.01) was used for data analysis and a Cy5.5 filter (excitation: 640 nm; emission: 710 nm) was used for the NIRF detection. The exposure time was 3 s and the field of view (FOV) was 25 × 25 cm. The whole body images were scanned at 0 (pre) and 24 h post-injection. At 24 h post-injection, lungs, heart, spleen, kidneys, and liver were dissected from the mice and their *ex vivo* images were also scanned.

2.5. Toxicity test

Female ICR mice (~20 g body weight; Samtako, Osan, Korea) were used to assess the lung toxicity of developed NPs after intravenous injection. Lungs were dissected from the mouse at 24 h post-injection of PLGA NPs and CS05-PLGA NPs. These samples were fixed with 4% (v/v) formaldehyde for 1 day and 6-μm sections were obtained for deparaffinization and hydration with ethanol. Using standard procedures, lungs were stained with hematoxylin and eosin (H&E).

2.6. Statistical analysis

All experiments were repeated at least three times and the data are shown as the mean ± standard deviation (SD). Statistical analysis was performed using two-tailed Student's *t*-test and analysis of variance (ANOVA).

3. Results and discussion

3.1. Preparation and characterization of NPs

Transient aggregation of CS-PLGA NPs in the blood stream, potentially leading to their improved accumulation in the lung capillaries for lung targeting, was demonstrated in this study. It was reported that drug carriers with micron size can move efficiently to lung tissue after intravenous injection [21]. However, injection of nanocarriers and spontaneous formation of aggregates in the blood stream for lung targeting have not been definitely studied. Adopted method may be facile, safe, and highly efficient strategy to accomplish lung targetability (Fig. 1).

PLGA NPs were fabricated by a modified emulsification-solvent evaporation method and CS was coated onto the outer surface of NPs for the preparation of CS-PLGA NPs [25,26]. As shown in Table 1, the mean diameters of CS02-PLGA NPs and CS05-PLGA NPs were greater than that of PLGA NPs. CS was coated to the outer surface of PLGA NPs, resulting in the significant increase in their mean diameter ($p < 0.05$). Narrow size distribution (around 0.2 polydispersity index) was maintained after CS coating of NPs. By CS coating, the negative zeta potential of PLGA NPs was shifted positively ($p < 0.05$). Electrostatic interaction between CS and PLGA seems to be responsible for the change in zeta potential values. Interestingly, CS05-PLGA NPs exhibited higher mean diameter and zeta potential value rather than CS02-PLGA NPs ($p < 0.05$).

Table 1
Characterization of NPs.

Formulation	Mean diameter (nm)	Polydispersity index	Zeta potential (mV)
PLGA NPs	225 ± 6	0.11 ± 0.02	−15 ± 1
CS02-PLGA NPs	264 ± 4*	0.17 ± 0.02	−7 ± 1*
CS05-PLGA NPs	338 ± 18*,#	0.23 ± 0.03	12 ± 1*,#

Data are presented as means ± SD ($n \geq 3$).
CS02-PLGA NPs and CS05-PLGA NPs indicate NPs coated with 0.2% (w/v) and 0.5% (w/v) CS, respectively.
* $p < 0.05$, compared with PLGA NPs group.
# $p < 0.05$, compared with CS02-PLGA NPs group.

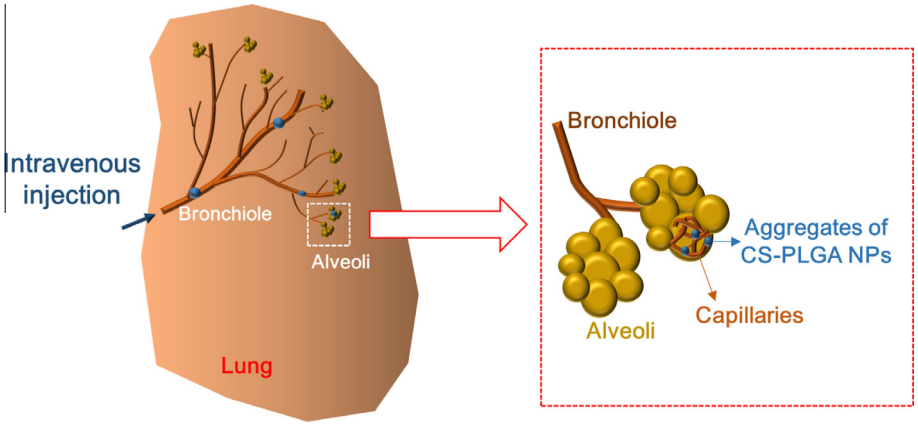

Fig. 1. Scheme of lung targeting strategy of CS-PLGA NPs.

Higher amount of CS seems to contribute to the increase of particle size and zeta potential value of NPs. Although 1% (w/v) CS was also coated to PLGA NPs in our preliminary study, that group was not included in this study due to their particle size (around 600 nm).

The mean diameter–time profiles of PLGA NPs, CS02-PLGA NPs, and CS05-PLGA NPs were monitored in different types of media (Fig. 2). When NPs are introduced into the blood stream, they may encounter diverse plasma proteins, which can be adsorbed to the surface of NPs [28]. Those protein coronas may govern the *in vivo* fate of NPs in the body. Adsorption of proteins in the surface of NPs is based on several types of forces, such as hydrogen

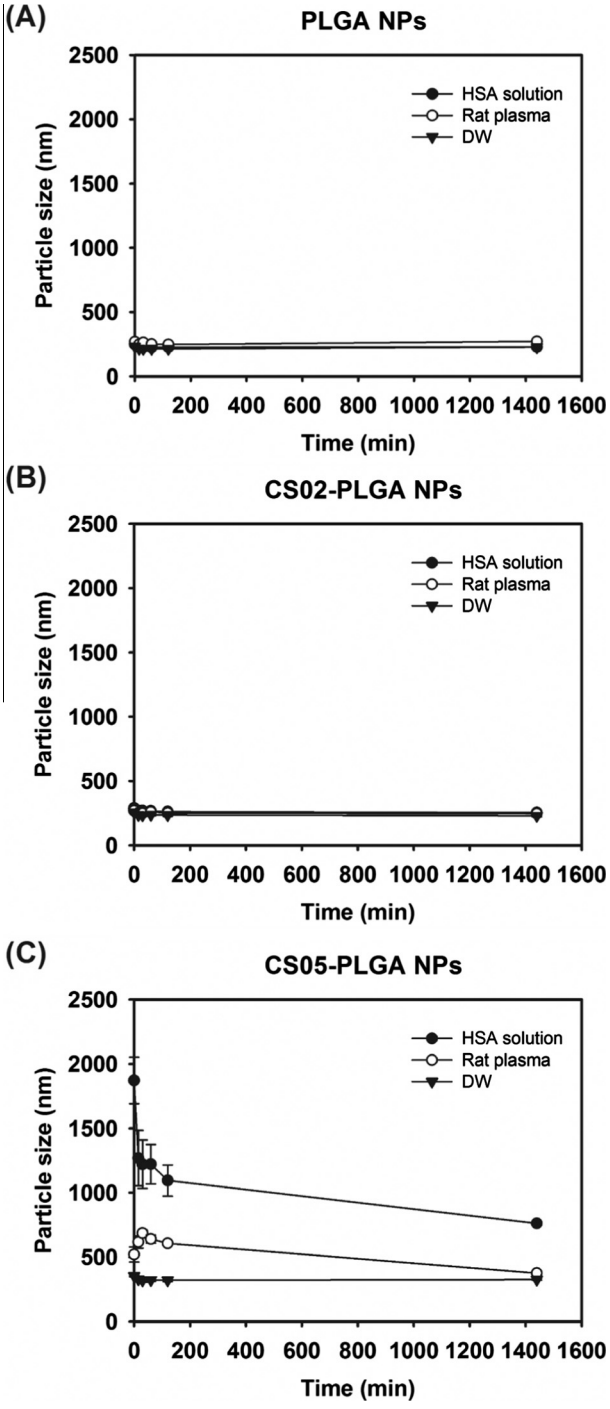

Fig. 2. *In vitro* stability of (A) PLGA NPs, (B) CS02-PLGA NPs, and (C) CS05-PLGA NPs in HSA solution, rat plasma, and DW. Particle size according to the incubation time was measured. Data are presented as the mean ± SD (n = 3).

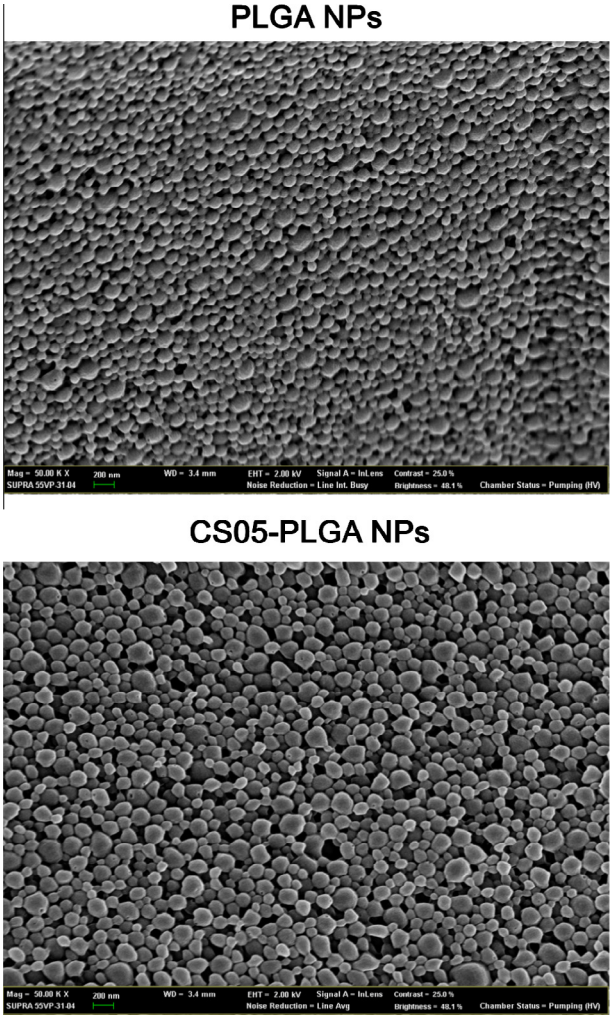

Fig. 3. FE-SEM images of PLGA NPs and CS05-PLGA NPs. The length of scale bar in the image is 200 nm.

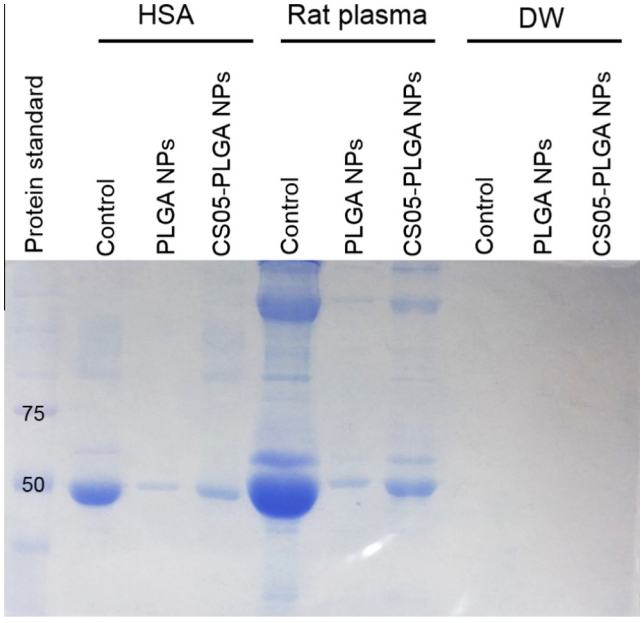

Fig. 4. The result of SDS-PAGE after incubating NPs in different media (HSA solution, rat plasma, and DW).

bonding, hydrophobic interactions, electrostatic interactions, and Van der Waals interactions [28,29]. Irreversibility or reversibility of protein binding to the surface of NPs can determine the characteristics of corona; hard *versus* soft [29]. It was reported that several proteins (*e.g.* albumin, fibrinogen chains, immunoglobulins, complement factors, plasminogen, and complement proteins) can adsorb on the surface of NPs prepared with different kinds of materials [29]. Of particular interest is that surface charge, hydrophobicity, size, morphology, shape, and surface curvature of NPs can affect the protein binding [28].

In this study, time-dependent particle size profiles of PLGA NPs, CS02-PLGA NPs, and CS05-PLGA NPs were measured in HSA solution, rat plasma, and DW (Fig. 2). PLGA NPs maintained their initial particle size in all types of media (HSA solution, rat plasma, and DW). CS02-PLGA NPs also exhibited constant mean diameter (< 300 nm) in those media. Although CS05-PLGA NPs exhibited nearly constant particle size in DW for 24 h, the particle size of CS05-PLGA NPs markedly increased in HSA solution and rat plasma. Interestingly, CS05-PLGA NPs in HSA solution exhibited 5.3-fold higher mean diameter compared with that value in DW after mixing with media ($p < 0.05$). However, the mean diameter of CS05-PLGA NPs was reduced at 24 h post-incubation. Similar pattern was also observed in rat plasma group. An electrostatic interaction between positively charged CS05-PLGA NPs and anionic plasma proteins seems to act as one of dominant forces in the transient aggregation of NPs. Notably, higher particle size in HSA group, rather than rat plasma group, seems to be based on the direct interaction between negatively charged HSA (isoelectric point [pI]: 4.7–4.9) in physiological pH and positively charged CS05-PLGA NPs. Diverse kinds of proteins with different physicochemical properties (*i.e.* pI value and molecular weight) included in rat plasma might hinder stronger electrostatic interaction as shown in HSA group. In addition, reduction of particle size of CS05-PLGA NPs was observed in HSA group within 15 min. Although we did not elucidate the detailed mechanism regarding it, the aggregates composed of HSA and CS05-PLGA NPs seemed to be dissociated in that incubation environment by several factors (*i.e.* intrusion of aqueous media into the aggregate and temperature). Immediate formation of micron size particles in HSA solution or rat plasma can increase their selective delivery to the lung. SEM images also provided similar particle size and uniform size distribution measured by DLS method (Fig. 3). Considering the transient aggregation of CS05-PLGA NPs compared with CS02-PLGA NPs, this group has been used in further studies.

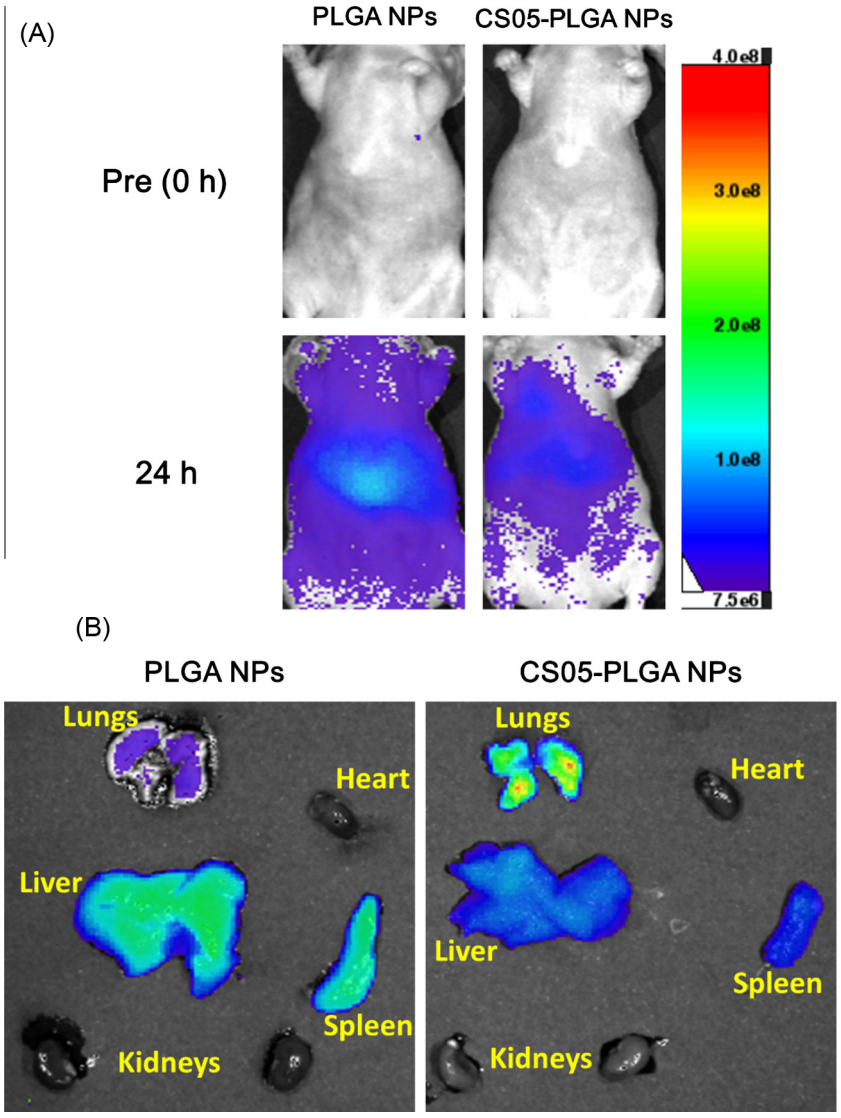

Fig. 5. NIRF imaging data after intravenous administration of PLGA NPs and CS05-PLGA NPs in the mouse. (A) *In vivo* imaging data are presented at 0 h (pre) and 24 h. (B) *Ex vivo* imaging data of lungs, heart, spleen, kidneys, and liver at 24 h post-injection are shown.

3.2. SDS-PAGE

Interactions between the NPs and serum proteins were investigated by SDS-PAGE analysis (Fig. 4). Adsorption of proteins to the surface of NPs was assessed by band intensity. In DW group, there was no protein band in control and NPs groups. On the while, in HSA solution and rat plasma groups, the control lane exhibited corresponding molecular weights of proteins. According to the quantitative analysis of band intensity, the relative ratios of PLGA NPs and CS05-PLGA NPs (compared with control group) after incubation with HSA solution were 6.6% and 23.7%, respectively. After incubation with rat plasma, those ratios of PLGA NPs and CS05-PLGA NPs were 3.3% and 17.1%, respectively. Regardless of the composition of media (HSA or rat plasma), CS05-PLGA NPs group had a higher degree of protein adsorption compared with PLGA NPs group.

In this study, it is assumed that mainly hydrophobicity and surface charge of NPs may affect their binding affinity with proteins. It is known that the extent of protein adsorption to the NPs may be higher in hydrophobic materials rather than in hydrophilic ones [30]. The surface charge is another factor which can explain the protein adsorption to the NPs. Positively charged NPs may adsorb proteins with pI < 5.5, whereby negatively charged NPs can adsorb proteins with pI > 5.5 [30]. Higher charge density on the outer surface can improve protein adsorption [31]. In this investigation, CS coating improved the hydrophilic property of NPs and it might induce less degree of protein adsorption compared with unmodified NPs. Nonetheless, surface charge type and density seemed to act as major roles in protein adsorption to NPs considering the observed results in Fig. 4. Higher protein binding rate of CS05-PLGA NPs, compared with PLGA NPs, may attribute to the formation of transient aggregates in the blood stream and the improved lung targetability.

3.3. NIRF imaging

Transient aggregate formation in the blood stream after intravenous injection and selective accumulation in the lung capillaries of CS05-PLGA NPs, compared with PLGA NPs, were investigated using a real-time NIRF imaging (Fig. 5). NIRF dye (Cy5.5) was encapsulated into the NPs and they were injected into normal mouse intravenously. As shown in Fig. 5A, PLGA NPs were mainly distributed in the liver while the distribution of CS05-PLGA NPs in the liver was not obvious at 24 h post-injection. Biodistribution of CS05-PLGA NPs, compared with that of PLGA NPs, was further studied by *ex vivo* NIRF imaging at 24 h post-injection (Fig. 5B). The relative ratios of fluorescence intensity of CS05-PLGA NPs group to PLGA NPs group were ordered as follows: liver ≈ spleen < kidneys ≈ heart < lungs. Compared with PLGA NPs group, CS05-PLGA NPs were principally accumulated in the lung. On the while, their distribution in the liver and spleen was lower than that of PLGA NPs group. Liver and spleen have been regarded as the major organs for the phagocytosis and elimination of foreign materials by mononuclear phagocyte system (MPS). The relative ratios of fluorescence intensity of lungs/(liver + spleen) were 0.12 and 0.56 in PLGA NPs and CS05-PLGA NPs groups, respectively. These results indicate that large amount of CS05-PLGA NPs seems to be distributed in the lung rather than liver and spleen, compared with PLGA NPs. By adopting a simple and facile strategy, such as coating NPs with CS (0.5% [w/v] in this study), efficient lung targeting of NPs was accomplished *via* the formation of transient aggregates in the blood stream.

It is reported that the capillary beds of several organs (*e.g.* lung, liver, and spleen) can be filters to capture MPs [21]. MPs with a higher diameter than that of capillary beds may be accumulated in those organs and this approach can be used as a passive targeting strategy. The biodistribution and toxicity of MPs are related to their size, dose, and rigidity. It was also known that particles with < 4 μm mean diameter may pass through the lung and deposit in the reticuloendothelial system (RES) of liver and spleen, while particles with > 10 μm mean diameter may principally distribute in the lung [21,32,33]. Although the internal diameter of pulmonary capillaries in mouse and the virtual size of aggregates of NPs in the blood stream were not measured in this study, the size of aggregates of NPs seems to be appropriate for their efficient distribution in the lung capillary of mouse.

3.4. Toxicity test

Toxicity of developed NPs on the lung epithelium was evaluated by H&E staining of dissected lung tissues (Fig. 6). Single injection of

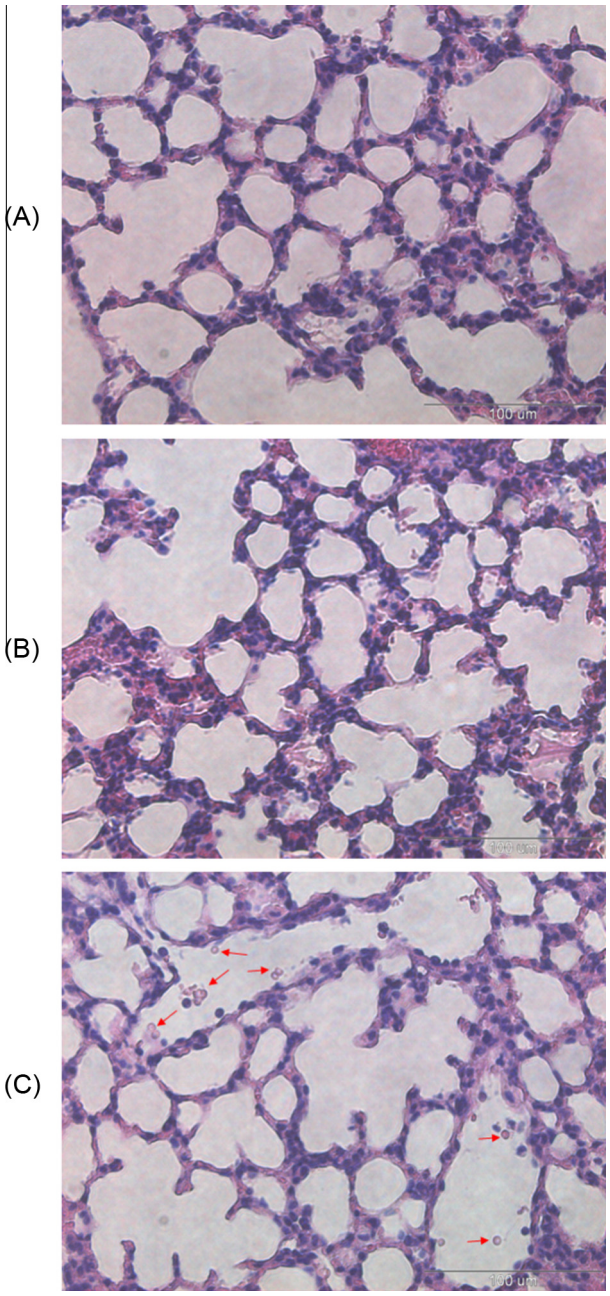

Fig. 6. Toxicity test of lung tissue after intravenous injection of NPs in mouse. H&E staining results of control (A), PLGA NPs (B), and CS05-PLGA NPs (C) are shown. Red arrows in the image of CS05-PLGA NPs group indicate the existence of micro-sized aggregates based on NPs. The length of bar in the image is 100 μm.

NPs *via* intravenous route did not induce severe toxicity in the lung epithelium. Micro-sized particles, based on the NPs, were frequently observed in the capillary beds of lungs in CS05-PLGA NPs, rather than those in control and PLGA NPs groups. This result is coincided with that of NIRF imaging study and it can support the higher lung targetability of CS05-PLGA NPs, compared with PLGA NPs, after intravenous injection.

It is known that micro-sized particles are prone to be accumulated in the capillary bed of the normal or tumor vasculature of the lung [21–23]. Micro-sized particles can block the blood stream and induce the embolization of the vasculature. But, temporarily formed aggregates based on NPs may be disassembled to individual NPs finally. Thus, their risk for embolization and subsequent toxicities may be lower than MPs [16]. Observed negligible toxicity of CS05-PLGA NPs can be explained by that mechanism.

4. Conclusions

In this investigation, lung targetability of CS05-PLGA NPs based on the transient aggregate formation was demonstrated. By coating PLGA NPs with CS (0.5%, w/v), the mean diameter increased slightly and the zeta potential was changed from negative to positive value. PLGA NPs maintained their initial particle size with incubation in HSA solution, rat plasma, and DW. However, CS05-PLGA NPs exhibited a marked increment of mean diameter after incubation in HSA solution and rat plasma. According to the result of SDS-PAGE assay, CS05-PLGA NPs group displayed higher plasma protein binding compared with PLGA NPs group. Higher accumulation of CS05-PLGA NPs in the lung, rather than the other organs and tissues, was elucidated by the optical imaging in the mouse. In our previous study [16], CS-PLGA NPs containing paclitaxel were developed and that group exhibited higher lung concentrations of drug in mice after intravenous injection, compared with unmodified PLGA NPs and Taxol groups. However, no direct evidence for improved lung targeting efficiency of CS-coated NPs was provided in that study [16]. In this investigation, *in vivo* fate and improved lung targetability of CS-PLGA NPs, compared with PLGA NPs, were demonstrated by protein adsorption and optical imaging studies. Moreover, transient formation of micro-sized aggregates composed of NPs may have less toxicity due to lower possibility of embolization, compared with MPs [16,21,24]. All these findings suggest that facile CS coating to NPs can provide the efficient lung targetability after intravenous injection. CS-PLGA NPs can be a promising candidate for injection formulations to treat lung diseases.

Acknowledgements

This research was supported by the National Research Foundation of Korea (NRF), funded by the Korean government (MSIP) (No. NRF-2015R1A1A1A05027671).

References

[1] M. Karimi, A. Ghasemi, P. Sahandi Zangabad, R. Rahighi, S.M. Moosavi Basri, H. Mirshekari, M. Amiri, Z. Shafaei Pishabad, A. Aslani, M. Bozorgomid, D. Ghosh, A. Beyzavi, A. Vaseghi, A.R. Aref, L. Haghani, S. Bahrami, M.R. Hamblin, Chem. Soc. Rev. 45 (2016) 1457.
[2] S.S. Lee, Y.B. Lee, I.J. Oh, J. Pharm. Invest. 45 (2016) 659.
[3] R. Lobenberg, J. Maas, J. Kreuter, J. Drug Target. 5 (1998) 171.
[4] E.M. Pridgen, F. Alexis, O.C. Farokhzad, Expert Opin. Drug Deliv. 12 (2015) 1459.
[5] K. Tahara, T. Sakai, H. Yamamoto, H. Takeuchi, Y. Kawashima, Int. J. Pharm. 354 (2008) 210.
[6] S.K. Sahoo, J. Panyam, S. Prabha, V. Labhasetwar, J. Control. Release 82 (2002) 105.
[7] L. Martin-Banderas, M. Durán-Lobato, I. Muñoz-Rubio, J. Alvarez-Fuentes, M. Fernández-Arevalo, M.A. Holgado, Mini Rev. Med. Chem. 13 (2013) 58.
[8] J.H. Park, J.Y. Lee, U. Termsarasab, I.S. Yoon, S.H. Ko, J.S. Shim, H.J. Cho, D.D. Kim, Int. J. Pharm. 473 (2014) 426.
[9] R. Dinarvand, N. Sepehri, S. Manoochehri, H. Rouhani, F. Atyabi, Int. J. Nanomedicine 6 (2011) 877.
[10] L. Chronopoulou, M. Massimi, M.F. Giardi, C. Cametti, L.C. Devirgiliis, M. Dentini, C. Palocci, Colloids Surf. B Biointerf. 103 (2013) 310.
[11] Y. Luo, Z. Teng, Y. Li, Q. Wang, Carbohydr. Polym. 122 (2015) 221.
[12] M. Wang, Y. Zhang, J. Feng, T. Gu, Q. Dong, X. Yang, Y. Sun, Y. Wu, Y. Chen, W. Kong, Int. J. Nanomedicine 8 (2013) 1141.
[13] K. Bowman, K.W. Leong, Int. J. Nanomedicine 1 (2006) 117.
[14] D. Gallez, J. Theor. Biol. 111 (1984) 323.
[15] N.G. Schipper, K.M. Vårum, P. Stenberg, G. Ocklind, H. Lennernäs, P. Artursson, Eur. J. Pharm. Sci. 8 (1999) 335.
[16] R. Yang, S.G. Yang, W.S. Shim, F. Cui, G. Cheng, I.W. Kim, D.D. Kim, S.J. Chung, C. K. Shim, J. Pharm. Sci. 98 (2009) 970.
[17] S.M. Hwang, D.D. Kim, S.J. Chung, C.K. Shim, J. Control. Release 129 (2008) 100.
[18] J.H. Park, H.E. Jin, D.D. Kim, S.J. Chung, W.S. Shim, C.K. Shim, Int. J. Pharm. 441 (2013) 562.
[19] S. Harsha, R.C.S. Rani, Int. J. Pharm. 380 (2009) 127.
[20] D. Huo, S. Deng, L. Li, J. Ji, Int. J. Pharm. 289 (2005) 63.
[21] H.L. Kutscher, P. Chao, M. Deshmukh, Y. Singh, P. Hu, L.B. Joseph, D.C. Reimer, S. Stein, D.L. Laskin, P.J. Sinko, J. Control. Release 143 (2010) 31.
[22] B. Lu, J.Q. Zhang, H. Yang, Int. J. Pharm. 265 (2003) 1.
[23] B. Lu, J.Q. Zhang, H. Yang, Drug. Deliv. 10 (2003) 87.
[24] H.L. Kutscher, P. Chao, M. Deshmukh, S. Sundara Rajan, Y. Singh, P. Hu, J.B. Joseph, S. Stein, D.L. Laskin, P.J. Sinko, Int. J. Pharm. 402 (2010) 64.
[25] J.Y. Lee, J.S. Kim, H.J. Cho, D.D. Kim, Int. J. Nanomedicine 9 (2014) 2803.
[26] I.S. Yoon, J.H. Park, H.J. Kang, J.H. Choe, M.S. Goh, D.D. Kim, H.J. Cho, Int. J. Pharm. 488 (2015) 70.
[27] U.K. Laemmli, Nature 227 (1970) 680.
[28] P. Aggarwal, J.B. Hall, C.B. McLeland, M.A. Dobrovolskaia, S.E. McNeil, Adv. Drug Deliv. Rev. 61 (2009) 428.
[29] S.R. Saptarshi, A. Duschl, A.L. Lopata, J. Nanobiotechnol. 11 (2013) 26.
[30] R. Gossmann, E. Fahrländer, M. Hummel, D. Mulac, J. Brockmeyer, K. Langer, Eur. J. Pharm. Biopharm. 93 (2015) 80.
[31] A. Gessner, A. Lieske, B. Paulke, R. Müller, Eur. J. Pharm. Biopharm. 54 (2002) 165.
[32] E.L. Dobson, H.B. Jones, Acta Med. Scand. Suppl. 273 (1952) 1.
[33] U. Scheffel, B.A. Rhodes, T.K. Natarajan, H.N. Wagner Jr., J. Nucl. Med. 13 (1972) 498.